

Article

Achieving Sustainable Development Goal 6 Electrochemical-Based Solution for Treating Groundwater Polluted by Fuel Station

Júlio César Oliveira da Silva ¹, Aline Maria Sales Solano ^{1,2,*}, Inalmar D. Barbosa Segundo ^{1,*} ,
Elisama Vieira dos Santos ^{1,3} , Carlos A. Martínez-Huitle ^{1,3,4,*}  and Djalma Ribeiro da Silva ¹

¹ Institute of Chemistry, Federal University of Rio Grande do Norte, Lagoa Nova, Natal 59078-970, RN, Brazil

² Federal Institute of Education, Science, and Technology of Rio Grande do Norte/Nova Cruz, Av. José Rodrigues de Aquino Filho, Nova Cruz 59215-000, RN, Brazil

³ National Institute for Alternative Technologies of Detection, Toxicological Evaluation and Removal of Micropollutants and Radioactives (INCT-DATREM), Institute of Chemistry, Universidad Estatal Paulista Júlio de Mesquita Filho, Araraquara 14800-900, SP, Brazil

⁴ Department Chemie, Johannes Gutenberg-Universität Mainz Duesbergweg 10-14, 55128 Mainz, Germany

* Correspondence: lininhamss@hotmail.com (A.M.S.S.); idbsegundo@gmail.com (I.D.B.S.); carlosmh@quimica.ufrn.br (C.A.M.-H.)



Citation: da Silva, J.C.O.; Solano, A.M.S.; Barbosa Segundo, I.D.; dos Santos, E.V.; Martínez-Huitle, C.A.; da Silva, D.R. Achieving Sustainable Development Goal 6 Electrochemical-Based Solution for Treating Groundwater Polluted by Fuel Station. *Water* **2022**, *14*, 2911. <https://doi.org/10.3390/w14182911>

Academic Editors: Dionysios (Dion) Demetriou Dionysiou, Yujue Wang and Huijiao Wang

Received: 6 August 2022

Accepted: 13 September 2022

Published: 17 September 2022

Publisher's Note: MDPI stays neutral with regard to jurisdictional claims in published maps and institutional affiliations.



Copyright: © 2022 by the authors. Licensee MDPI, Basel, Switzerland. This article is an open access article distributed under the terms and conditions of the Creative Commons Attribution (CC BY) license (<https://creativecommons.org/licenses/by/4.0/>).

Abstract: Oil leakage occurs at fuel service stations due to improper storage, which pollutes soil and, subsequently, can reach the groundwater. Many compounds of petroleum-derived fuels pose hazards to aquatic systems, and so must be treated to guarantee clean and safe consumption, which is a right proposed by the United Nations in their Sustainable Development Goal 6 (SDG 6: Clean Water and Sanitation). In this study, contaminated groundwater with emerging pollutants by petroleum-derived fuel was electrochemically treated in constantly mixed 0.5 L samples using three different anodes: Ni/BDD, Ti/Pt, Ti/RuO₂. Parameters were investigated according to chemical oxygen demand (COD), energy consumption analysis, by applying different electrodes, current densities (*j*), time, and the use of Na₂SO₄ as an electrolyte. Despite a similar COD decrease, better degradation was achieved after 240 min of electrochemical treatment at Ti/RuO₂ system (almost 70%) by applying 30 mA cm⁻², even without electrolyte. Furthermore, energy consumption was lower with the RuO₂ anode, and greater when 0.5 M of Na₂SO₄ was added; while the order, when compared with the other electrocatalytic materials, was Ti/RuO₂ > Ti/Pt > Ni/BDD. Thereafter, aiming to verify the viability of treatment at a large scale, a pilot flow plant with a capacity of 5 L was used, with a double-sided Ti/RuO₂ as the anode, and two stainless steel cathodes. The optimal conditions for the effective treatment of the polluted water were a *j* of 30 mA cm⁻², and 0.5 M of Na₂SO₄, resulting in 68% degradation after 300 min, with almost complete removal of BTEX compounds (benzene, toluene, ethyl-benzene, and xylene, which are found in emerging pollutants) from the water and other toxic compounds. These significant results proved that the technology used here could be an effective SDG 6 electrochemical-based solution for the treatment of groundwater, seeking to improve the quality of water, removing contaminants, and focusing on Brazilian environmental legislations and, consequently, converting pollutants into effluent that can be returned to the water cycle.

Keywords: anodic oxidation; BTEX; groundwater pollution; electrochemical oxidation; sustainable development goals

1. Introduction

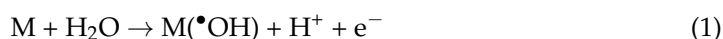
Groundwater refers to any amount of water located below the earth's surface, constituting an important water reserve for consumption, mainly for regions where there are waterbodies unable to meet the needs of the population [1]. The importance of preserving and/or recovering these water systems is essential for both the current society and future

generations in order to accomplish the Sustainable Development Goals (SDGs) proposed by the United Nations (UN). SDG 6 regards ensuring availability and sustainable management of water and sanitation for all, seeking to attend not only drinking water, but also water harvesting, water efficiency, desalination, wastewater treatment, recycling, and reuse technologies [2]. According to the UN, the way to promote this goal by 2030 is through the implementation of the following targets: (i) to achieve safe and affordable drinking water; (ii) sanitation and hygiene and end open defecation; (iii) improve water quality, wastewater treatment, and safe reuse; (iv) increase water-use efficiency and ensure freshwater supplies; (v) implement integrated water resources management; and (vi) protect and restore water-related ecosystems [3].

However, several industrial and human activities (e.g., population growth, the increasing demand for energy consumption, the exploitation of natural resources, and the inappropriate disposal or storage of products harmful to human health) have caused significant pollution problems, such as the contamination of rivers and groundwater, subsequently provoking negative environmental impacts that can affect the whole ecosystem [4]. Some recalcitrant and hazardous contaminants such as polycyclic aromatic hydrocarbon (PAH), polychlorinated biphenyl (PCB) [5], BTEX compounds [6], and trichloroethylene [7] are frequently identified in polluted groundwater.

Conventional water treatment methods (wet-air oxidation, Fenton type processes, super critical water oxidation, photocatalysis, adsorption, etc.) attend to the problems related to SDG 6 in several sectors, but sometimes these approaches can be operationally intensive, chemically severe, and energetically expensive. Therefore, the design and development of environmentally innovative SDG 6 solutions [8,9] have been significantly stimulated. In the last years, electrochemical advanced oxidation technologies have received great attention because these processes are considered feasible alternatives to prevent or solve many environmental problems related to water pollution [10,11]. At the same time, the use of renewable technologies as the main electrical energy source, instead of the conventional electrical supply, has extended the applicability of these approaches in different water-security sectors [12,13].

This type of SDG 6 technology efficiently eliminates a great number of persistent organic pollutants [14–16] and microorganisms by promoting the in-situ electrogeneration of oxidizing species. Among the SDG 6 electrochemical-based solutions, anodic oxidation (AO) or electrooxidation (EO) is the most popular approach to be considered since it is a robust, easy, safe, and eco-friendly water treatment solution [15,16]. Based on their electrocatalytic fundamentals, AO can follow two ways on the oxidation of organic pollutants at the anodic surface (M) by direct electron transfer and/or more quickly by the reaction with the $\bullet\text{OH}$ which were formed from the oxidation of water (Equation (1)) [15,17,18]:



The amount of the electrogenerated heterogenous free $\bullet\text{OH}$ depends on the electrocatalytic material used, like active (e.g., Pt, IrO₂, and RuO₂) and non-active (e.g., PbO₂, SnO₂, and boron-doped diamond (BDD)), favoring the conversion of organics into by-products (due to lower amounts of free $\bullet\text{OH}$, occurring direct oxidation) or promoting the complete incineration of pollutants to CO₂ and water (due to the higher amount of free $\bullet\text{OH}$, once indirect oxidation takes place) [10,19,20]. Although non-active anodes are frequently used because they are more effective to degrade different pollutants (ranging from $\mu\text{g L}^{-1}$ to g L^{-1} [16,21]) in various water matrices [22–26], significant advances in strategies for preparing/synthesizing novel electrocatalytic materials have been achieved to replace non-active anodes [26,27] as well as to develop/design innovative electrochemical reactors aiming to successfully translate from laboratory cells to pilot scale-up [28,29].

Therefore, this work aims to evaluate the efficiency of the electrochemical degradation of groundwater contaminated by fuel leak underneath a gas station at different anodic materials (Ti/RuO₂, Ti/Pt, and NB/BDD), in a batch stirring cell, applying 10, 30, and 60 mA cm^{-2} at 25 °C. After that, an electrocatalytic material was selected to scale up

the electrochemical system aiming to study the effective assessment of the water quality with an innovative SDG 6 electrochemical-based solution to treat 5 L of fuel polluted-groundwater using a reactor with 286 cm² of geometrical area. The scaling up of the electrochemical device intends to prove that this technology could be an effective solution for water treatment, fulfilling SDG 6 via the improvement of the quality of water and returning it to the water cycle.

2. Materials and Methods

2.1. Characterization of Groundwater Effluent

The yellowish groundwater sample was collected in areas of fuel recovery stations in Natal city, in the northeastern Brazilian region, by trained technicians of the Universidade Federal do Rio Grande do Norte, approximately 10 m below the water level, and removing the supernatant oil. Different chemical compounds in the collected sample were identified and quantified by gas chromatography—mass spectroscopy (GC—MS) technique using commercially available standard compounds. EPA standard method 8021 was used to evaluate the sample by GC with a serial detector CG-PID/FID, column OV624 (gas flow: 3.0 mL min⁻¹), with initial temperature of 40.15 °C/1.0 min, after 10 °C/min to 150 °C, with a total analysis time of 32 min. Split-less injector temperature was 250 °C, lamp temperature (PID) was 280 °C, and detector FID was 300 °C. Before the GC—MS analysis, the samples were treated by solid-phase micro-extraction (SPME) with an 85 µm film of poly-(dimethylsiloxane) fiber. Once the extraction was completed (10 min), the fiber was withdrawn back inside the fiber holder, removed from the reaction sample, and then injected by a 1:25 split method. The temperature of the transfer line was 240 °C, the ions trap was 170 °C, and the desorption time in the split-less mode at 260 °C was 3 min. Other physical-chemical characteristics were also measured (Table 1).

2.2. EO Experiments

Two electrochemical reactors were used to perform the bulk-electrolysis: (i) a conventional laboratory cell with a capacity of 0.5 L (Figure 1a) and (ii) an electrochemical pilot flow cell with a capacity of 5 L (Figure 1b). In the former, AO experiments were carried out under galvanostatic conditions using a MINIPA MPL-3305M power supply with Ti/Pt, Ti/RuO₂, or Nb/BDD as anodes, and a titanium plate as the cathode (each one of them with a geometrical area of 13.5 cm²; and an electrode-gap of 1.5 cm) by applying 10, 30, and 60 mA cm⁻² at 25 °C; while an electrochemical flow cell with a double-sided RuO₂ anode and two stainless steel plates as the cathodes (each one of them with a geometrical area of about 286 cm⁻² and electrode-gaps of 3 cm) were used for electrochemically treating polluted-groundwater effluent, which was recirculated by the pilot plant using a pump with a flow rate of 153 L h⁻¹, by applying 30 mA cm⁻² at 25 °C (experimental conditions were established by the preliminary experiments with batch cell) in the latter.

2.3. Analytical Methods

Polluted-groundwater decontamination was monitored from its chemical oxygen demand (COD) and total organic carbon (TOC) reductions, determined on a Hanna Instruments HI 83399 multiparameter photometer and TOC analyzer (Analytik Jena model multi-N/C 3100, by injecting 30 mL aliquots), respectively. On the one hand, COD measurements were determined by using 2 mL of effluent sample in pre-prepared kit HANNA solutions which remained 2 h under the digestion process at 150 °C into a thermo-reactor (HANNA model HI 839800). On the other hand, BOD₅ was measured using an OxiTop[®] system (manometric respirometry). Another method for organic analysis is according to the specific ultraviolet absorbance at 254 nm (SUVA₂₅₄, L mg⁻¹ m⁻¹), which can be used as an indicator of aromaticity and chemical reactivity for aquatic organic matter samples from a wide range of water sources. It is obtained by dividing the UV absorbance at 254 nm (m⁻¹) of samples by TOC values (mg L⁻¹) [30]. Finally, pH conditions were monitored

using a Nova Instruments pH-meter HANNA and the conductivity was measured with an Electrical Conductivity meter model HI4321.

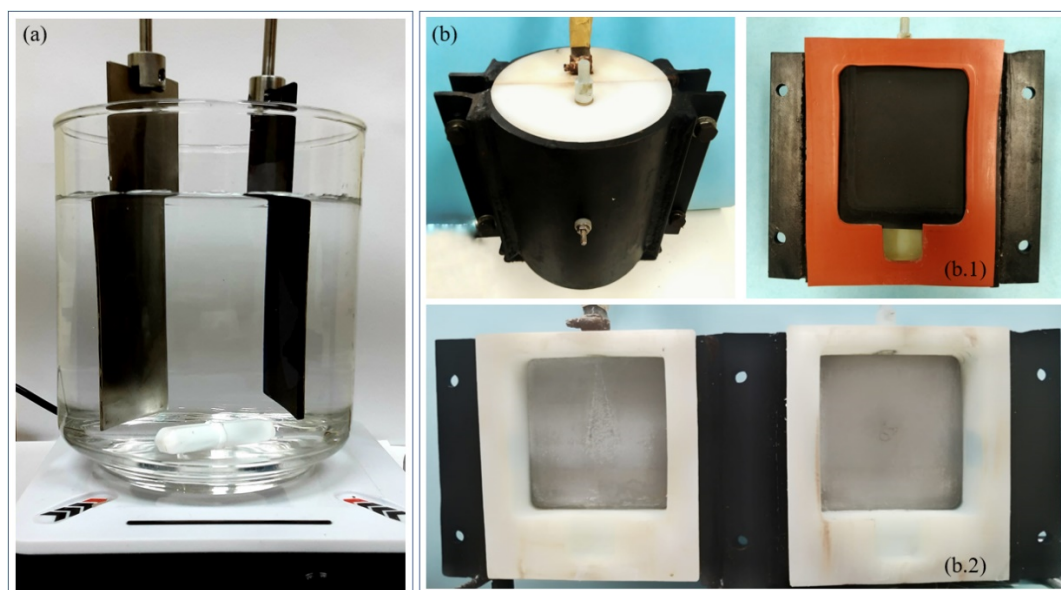


Figure 1. Electrochemical reactors: batch mode (a) and the flow cell (b) with the Ti/RuO₂ anode placed in the middle of the reactor (b.1), and the opened reactor detailing the two stainless steel plates as cathodes.

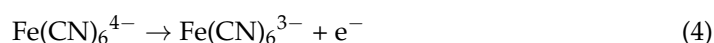
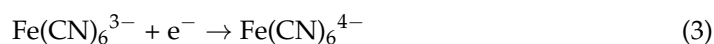
The discoloration was determined by measuring the absorbance reduction with a Shimadzu UV 1800 spectrophotometer during the AO tests of groundwater effluent at different applied current densities. Wavelength peaks at 436, 525, and 620 nm were taken from the UV-Vis spectrum between 200–800 nm, and then DFZy calculation was made according to Equation (2) following the method DIN EN 7884:2012 [31].

$$DFZ_y = 100 \times \left(\frac{E_y}{d} \right) \quad (2)$$

where E_y is the absorbance at a y wavelength and d is the cell path length in cm.

2.4. Electrochemical Flow Reactor Characterization

The electrochemical flow reactor was hydrodynamically characterized by the limiting diffusion current technique. Potassium ferricyanide ($K_4Fe(CN)_6$) solutions, ranging from 20 to 80 mmol L⁻¹ in 0.5 mol L⁻¹ NaOH, were electrolyzed with a flow rate of 153 L h⁻¹, and the potential-current profiles for the oxidation-reduction reactions (Equations (3) and (4)) were determined by increasing the voltage stepwise.



Then, polarization curves were obtained and plotted to estimate the limiting currents at each one of the ferricyanide ($K_4Fe(CN)_6$) solutions at different concentrations [32]. From the slope value obtained by the profile limiting current vs. redox couple concentration, the mass-transfer coefficient of the reactor was estimated by Equation (5).

$$k_m = \frac{i_L}{zFAC_\infty} \quad (5)$$

k_m is the mass-transfer coefficient (m s^{-1}), i_L is the electrolysis limiting current (A), z is the electrons transfer in the redox reaction (for this redox pair, 1), F is the Faraday constant ($96,487 \text{ C mol}^{-1}$), A is the electrode surface area (m^2), and C_∞ is the bulk species concentration (mol dm^{-3}).

3. Results

3.1. Effluent Characterization

GC—MS results (see Table 1) showed that the concentrations of benzene, toluene, ethylbenzene, xylene (called BTEX), and phenol in the groundwater collected-sample were higher than the maximum allowed for human consumption, as well as 230 mg L^{-1} of COD. Furthermore, other physical characteristics were measured and reported in Table 1.

3.2. Influence of the Applied j and the Effect of Different Anode Materials Using the Batch Reactor

Electrocatalytic material and current density (j) are two of the main operating parameters that determine the effectiveness of the decontamination of water matrices by electrochemical advanced oxidation processes (EAOPs). A higher concentration of oxidizing species can be electrochemically generated, and higher pollutant degradation can be attained, depending on the anode and j selected. Therefore, it is essential to study the anodic material and j effects in order to determine the degradation efficiency of the SDG 6 electrochemical-based solution proposed here, since there are electrodes and j values that promote undesirable parasitic reactions, leading to similar or even lower pollutant removal [33]. To do that, Ti/RuO₂, Ti/Pt, or Nb/BDD anode were used in a batch reactor to investigate the effect of the j on the EO of groundwater by applying 10, 30, and 60 mA cm^{-2} at 25 °C.

Table 1. Physical-chemical characterization before EO treatment of groundwater collected sample.

Parameter	Before Treatment	MAV ^a
pH	6.59	-
Conductivity (mS cm^{-1})	0.292	-
Phenol content ($\mu\text{g L}^{-1}$)	6	3
Benzene ($\mu\text{g L}^{-1}$)	96.6	5
Toluene ($\mu\text{g L}^{-1}$)	2441	170
Ethylbenzene ($\mu\text{g L}^{-1}$)	925.5	200
Xylene (<i>o</i> -, <i>p</i> - and <i>m</i> -) ($\mu\text{g L}^{-1}$)	5435.5	300
BOD (mg L^{-1})	80.5	-
COD (mg L^{-1})	230	-
TOC (mg L^{-1})	91.5	-
Total petroleum hydrocarbons (TPHs) (mg L^{-1})	4.66	-
Color (DFZ at 436, 525, and 620 nm, respectively)	9.5, 6.5, 4.9	-
Absorbance at 254 nm (AU)	0.714	-
SUVA ₂₅₄	0.78	-
Turbidity (NTU)	7.9	-

Note: ^a Maximum allowed value for groundwater (human consumption) based on current legislation in Brazil [34].

Figures 2 and 3 show that both factors (type of electrode and j) significantly influence the COD decay, using a batch stirring reactor with 0.5 L of effluent (the lines represent the trend of the symbols, which are the real values). As can be observed, no complete organic

matter removal was attained independently of the anodic material and j , respectively. By applying 30 mA cm^{-2} , 78.3%, 81%, and 78.2% of COD removals were achieved at Ti/RuO₂, Ti/Pt, and Nb/BDD anodes, respectively. Meanwhile, COD removals of about 75.6% and 77% were reached for Ti/RuO₂ and Ti/Pt, respectively, by applying 60 mA cm^{-2} . This decrease in efficacy was associated with the promotion of the oxygen evolution reaction over organics oxidation at higher j due to the anodic electrode used, such as Ti/RuO₂ and Ti/Pt, which are considered active anodes. Conversely, ineffective COD removals were achieved at 10 mA cm^{-2} because a lower concentration of free $\bullet\text{OH}$ radicals is produced at Ti/RuO₂ and Ti/Pt electrodes. COD results preliminarily evidenced that the process is potentially controlled by mass transport conditions at all electrocatalytic materials because of the concentration of pollutants, type of electrocatalytic material, undesired reactions at higher j (e.g., oxygen evolution reaction), and the flow-hydrodynamic cell conditions. Nevertheless, the mass transport conditions affecting the process at Ti/RuO₂ and Ti/Pt electrodes seem to be more significant than diamond electrode. In fact, COD removal increased approximately 4.2% and 10.1% by applying 60 mA cm^{-2} from the removal efficiencies achieved at 30 and 10 mA cm^{-2} , respectively, when the BDD electrode was used. This behavior is due to the physisorbed $\bullet\text{OH}$, which are efficiently electrogenerated via water discharge (Equation (1)) at the non-active diamond surface, and confined close to the anode surface in the reaction cage, favoring the degradation of organic matter and, consequently, achieving the best oxidation performances compared with the others [35,36].

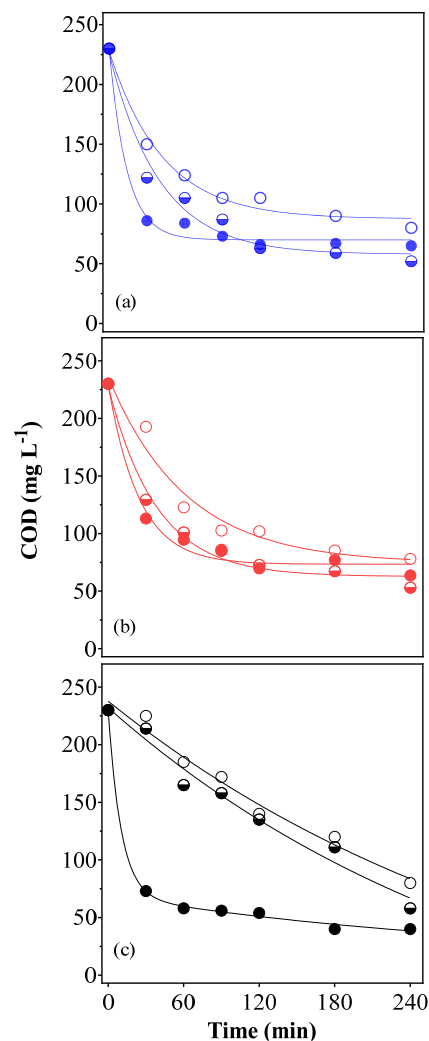


Figure 2. Influence of 10, 30, and 60 mA cm^{-2} (empty, half-, and full-colored, respectively), as a function of time on the COD removal during the EO: (a) Ti/RuO₂, (b) Ti/Pt, and (c) Nb/BDD.

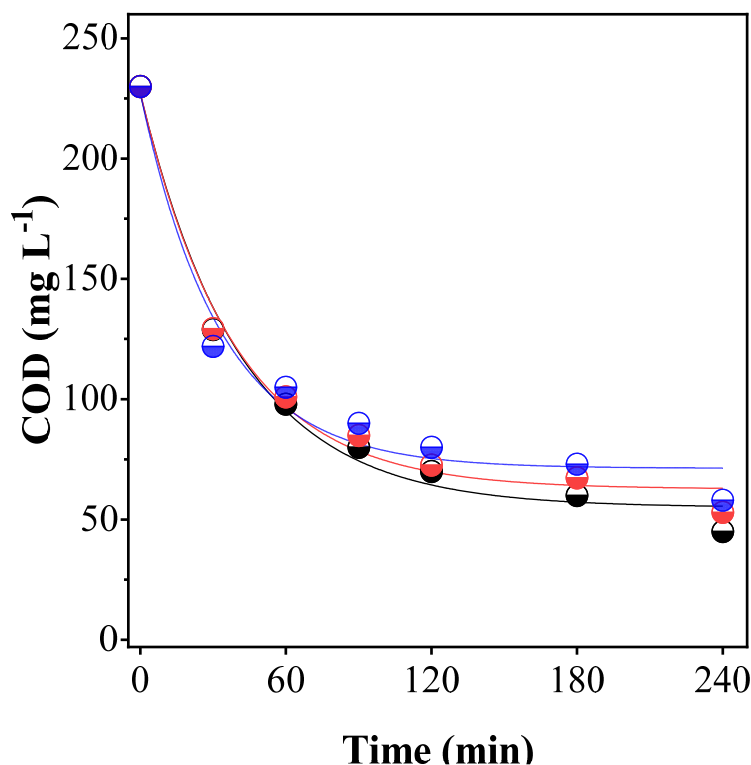


Figure 3. Influence of the electrocatalytic material (Ti/RuO₂ ●; Ti/Pt ●; Nb/BDD ●) on COD decay as a function of time, when Na₂SO₄ was added to the real water matrix by applying 30 mA cm⁻² at 25 °C.

The results have indicated that the degradation of the pollutants present in the effluent was mainly controlled by mass transport in several cases (at Ti/RuO₂, Ti/Pt, and Nb/BDD anodes) because, independently of the j and the exponential, COD decayed at the beginning of the electrolysis; it remained almost stable in the last 150 min of the treatment. This behavior was also confirmed by the estimation of the limiting current (I_{lim}) value, considering the initial COD as well as the hydrodynamic conditions of the batch cell (Equation (5)), as already reported in our previous work.

$$I_{lim}(t) = 4FAk_m \text{COD}(t) \quad (6)$$

where $I_{lim}(t)$ is the limiting current (A) at a given time t , 4 is the number of exchanged electrons, A is the electrode area (m²), F is the Faraday's constant, k_m is the average mass transport coefficient in the electrochemical reactor (m s⁻¹), and $\text{COD}(t)$ is the chemical oxygen demand (mol O₂ m⁻³) at a given time t .

An I_{lim} of 0.11 A was estimated, considering a k_m of 1.9×10^{-5} m s⁻¹. This current value is lower than all the currents applied in this work (0.14, 0.41, and 0.82 A for 10, 30, and 60 mA cm⁻², respectively), confirming that the AO technology, under these conditions, is taking place under mass transport control. On the other hand, I_{lim} of 0.11 A is significantly lower than 0.81 (value estimated for the j of 60 mA cm⁻²), which explains the fact that there was not a significant enhancement at higher j , as a consequence of a higher charge which was consumed in parasite non-oxidizing reactions such as oxygen evolution. These assumptions, treating a real water matrix, are in agreement with various studies [37–39] about the EO of real wastewater. Based on the results obtained, a j of 30 mA cm⁻² was selected as the optimum value to be applied in a new set of experiments by adding Na₂SO₄ as a supporting electrolyte where the effects of the reduction of COD were studied with Ti/RuO₂, Ti/Pt, and Nb/BDD anodes.

3.3. Comparative Groundwater EO Using Different Anodes Adding Sulfate as Supporting Electrolyte

In accordance with other studies [40–42], the addition of salts such as NaCl or Na₂SO₄ in real effluent favors an increase in conductivity, having a positive effect on the degradation of organic matter. On the one hand, the water discharge is favored (Equation (1)), producing •OH; while, on the other hand, the electrogeneration of additional oxidizing species is promoted by the oxidation of salt precursors, such as NaCl or Na₂SO₄ [43], enhancing the elimination of pollutants from water matrix. In this sense, a known amount of Na₂SO₄ was added to 0.5 L achieving a concentration of about 0.5 M.

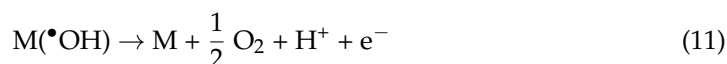
In the case of Ti/RuO₂ and Ti/Pt, •OH are strongly adsorbed on their surfaces, higher oxides are formed (Equation (7)), which participate as a mediator (Equation (8)) in the selective oxidation of organics, R (so-called electrochemical conversion), which occurs in concomitance with oxygen evolution (Equation (9)), as a side reaction, affecting the efficiency of the EO process.



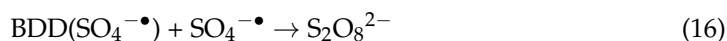
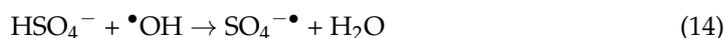
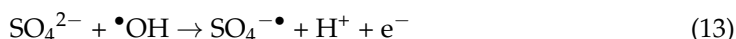
In this sense, direct electrochemical oxidation at Ti/RuO₂ and Ti/Pt surfaces is preferentially favored (direct electron transfer from the organics to the anode surface), limiting the effectiveness of the process. Conversely, when the Nb/BDD anode is used, the •OH are weakly adsorbed on its surface, rapidly reacting with the organic molecules, consequently leading to electrochemical incineration (CO₂, and water (Equation (10))).



This reaction also competes with the side reaction of O₂ evolution (Equation (11)), which can significantly affect the efficiency of the electrolytic treatment.



Considering the information above and the results in Figure 4, the partial elimination of COD in all electrodes is a consequence of the formation of byproducts during the electrochemical treatment of the real water matrix by applying 30 mA cm⁻², even when the effluent conductivity was increased due to the addition of Na₂SO₄. Additionally, the promotion of the oxygen evolution reaction (Equation (9)), as an undesired reaction, can be favored at Ti/RuO₂ and Ti/Pt electrodes when the conductivity is increased, consequently limiting the elimination of organics. Meanwhile, the slight organics removal improvement of the effluent when BDD was used and Na₂SO₄ added could be associated with the electrochemical production of sulfate-based oxidants, such as SO₄^{•-} and S₂O₈²⁻. Their formation, via direct or indirect electrosynthetic routes, depends on the BDD surface properties, electrolyte medium, its concentration, and the current or potential applied [44–47] (Equations (12)–(16)).



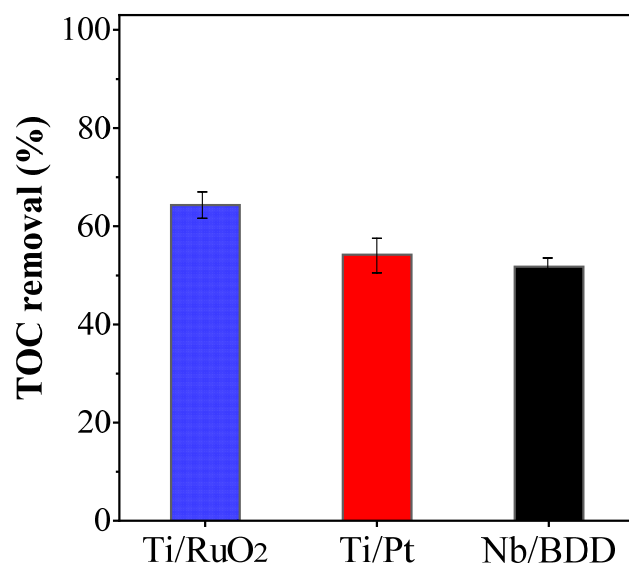


Figure 4. TOC removals, as a function of electrocatalytic material, when no Na₂SO₄ was added to real water matrix by applying 30 mA cm⁻² at 25 °C.

This mix of oxidants remains at the reaction cage (BDD-•OH/SO₄•⁻/S₂O₈²⁻), oxidizing several organic pollutants in different water matrices [44,48], deactivating microorganisms [47,49], and depolluting soil matrices (by using soil washing, electrokinetic soil remediation, or soil flushing) [50,51]. However, ionic species in the water matrices could act as scavengers, trapping the oxidants and, consequently, reducing their oxidative action [24,52], like Cl⁻, HCO₃²⁻, and others. Therefore, the effectiveness of the process was also evaluated by the organic matter degradation (COD) and mineralization (TOC).

In terms of COD removal, as can be observed in Figure 3, no significant removals were achieved (ranging from 75–80%) by applying 30 mA cm⁻² when sulfate was added in the effluent. Comparable efficiencies were achieved without the addition of sulfate in the effluent (78.26%, 81%, and 78.2% of COD removals were achieved at Ti/RuO₂, Ti/Pt, and Nb/BDD anodes, respectively), under similar experimental conditions. Nevertheless, some differences were observed when the mineralization removal was determined by TOC measurements (Figure 4). As can be observed, Ti/RuO₂ anode efficiently mineralized the organic matter, reaching approximately 64.61%. Meanwhile, Ti/Pt and Nb/BDD anodes achieved about 54.20 and 51.74% of TOC removals, respectively. This behavior can be associated with the electrode deactivation of surface and oxidants scavengers. In the former, Pt surface can be deactivated due to the adsorption of BTEX compounds or their oxidation byproducts [42]; while the oxidants electrogenerated at BDD could be trapped by the scavenger species in the water matrix, in the latter. Conversely, the enhancement on the mineralization at Ti/RuO₂ can be related to the occurrence of direct electrochemical oxidation of organics and byproducts at its surface (without surface deactivation), in concomitance with the oxygen evolution reaction.

Thus, with these results, and aiming to understand the energy requirements needed in terms of kWh gCOD⁻¹ to evaluate the feasibility of the process, energy consumption was estimated by using Equation (17).

$$EC \text{ (kWh (gCOD)}^{-1}) = (E_{\text{cell}} \times I \times t) / (\Delta(\text{COD})_{\text{exp}} \times V_s) \quad (17)$$

where V_s is the solution volume (L), I refers to the current intensity (A), $\Delta(\text{COD})_{\text{exp}}$ (g O₂ L⁻¹) refers to the difference between initial COD and COD at time t , t to the electrolysis time in hours, and E_{cell} to the average potential difference of the cell (V). Table 2 reports the EC values for all experimental conditions, in the absence and presence of sulfate in the effluent.

Table 2. Energy consumption values (kWh gCOD^{-1}), as a function of j and electrocatalytic material, after 240 min of electrochemical treatment, adding or not adding Na_2SO_4 in the effluent, and considering approximately between 75–80% of COD removal.

Electrode	j (mA cm^{-2})			
	10 ^a	30 ^a	60 ^a	30 ^b
Ti/RuO ₂	0.023	0.068	0.174	0.050
Ti/Pt	0.020	0.073	0.195	0.068
Nb/BDD	0.028	0.098	0.272	0.085

Note: ^a without Na_2SO_4 , ^b with Na_2SO_4 .

It was possible to observe that, as the j was increased, the energy consumption significantly increased. After 240 min of EO, the tests with Ti/RuO₂ adding Na_2SO_4 (COD removal = 75%) and without Na_2SO_4 (COD removal = 78%) lead to lower energy consumptions of 0.068 and 0.050 kWh kgCOD^{-1} , respectively, by applying 30 mA cm^{-2} . Meanwhile, for the experiments using Ti/Pt and Nb/BDD, in the presence and absence of sulfate, more substantial electrical requirements are needed to achieve at least 78% of organic matter removal. Although the EO experiments with BDD seem to be optimal in terms of organic matter removal, the use of oxide-based electrodes could be more eco-technologically suitable.

Another feature that should be considered is that the two-electrode cell operating under galvanostatic mode serves to provide only general information about the electrical requirements of each EO assay and, consequently, the economic costs. Although this cell option has specific benefits, it could offer apparent experimental conditions that are not reproducible and not completely fixed; consequently, the EO behavior is difficult to be scaled. In this sense, an electrochemical flow reactor is the most appropriate strategy to scale up the water SDG 6 solution because it allows for improving the electrode size, batch recirculation mode operation, the use of more economic electrode materials and shapes, and their components are suitable to be produced in large amounts. For this reason, Ti/RuO₂ electrode was chosen for upgrading the EO process.

3.4. EO of Groundwater at the Pre-Pilot Plant

The mass transfer characterization of the pre-pilot plant was firstly performed (Figure 1). Then, the polarization curves (current response vs. voltage) were registered during electrolysis, in the electrochemical flow reactor, of different solutions of ferricyanide (i.e., 20–80 mol m^{-3}) in 0.5 mol L^{-1} NaOH at a constant flow rate of $4.25 \times 10^{-5} \text{ m}^3 \text{ s}^{-1}$. As can be observed from Figure 5, well-defined limiting current-profiles were achieved at all polarization curves. It is clear that the limiting current increased when an increase in the concentration of ferricyanide solution was attained. This behavior indicated that the mass transfer rate at the electrode surface depends on the concentration of ions in the electrolyte. By plotting the limiting current profiles, as a function of the ferricyanide concentration, a linear relationship was reached (inset in Figure 5) and, consequently, the experimental k_m was estimated by Equation (5).

Mass-transfer rate was approximately $8.8 \times 10^{-6} \text{ m s}^{-1}$; this shows that the design allowed a good migration of ferricyanide ions towards the electrode surface during electrolysis due to its design and hydrodynamic conditions. However, the value of k_m obtained with the batch cell was slightly higher than the pre-pilot plant (1.9×10^{-5} and $8.8 \times 10^{-6} \text{ m s}^{-1}$, for batch and flow cells, respectively), reaching better mass transfer in the former configuration. This behavior is completely associated with the residence-solution time on the reaction compartment, which is lesser at the pre-pilot plant than that probably attained at the batch cell. It is important to also state here that the treated-effluent volume is different at both cells, and it significantly influences the k_m as well as the hydrodynamic reactor configuration. In the electrochemical flow cell, the variation of k_m may not necessarily result in significant treatment efficiency for complex organics dissolved in the groundwater polluted by the fuel station.

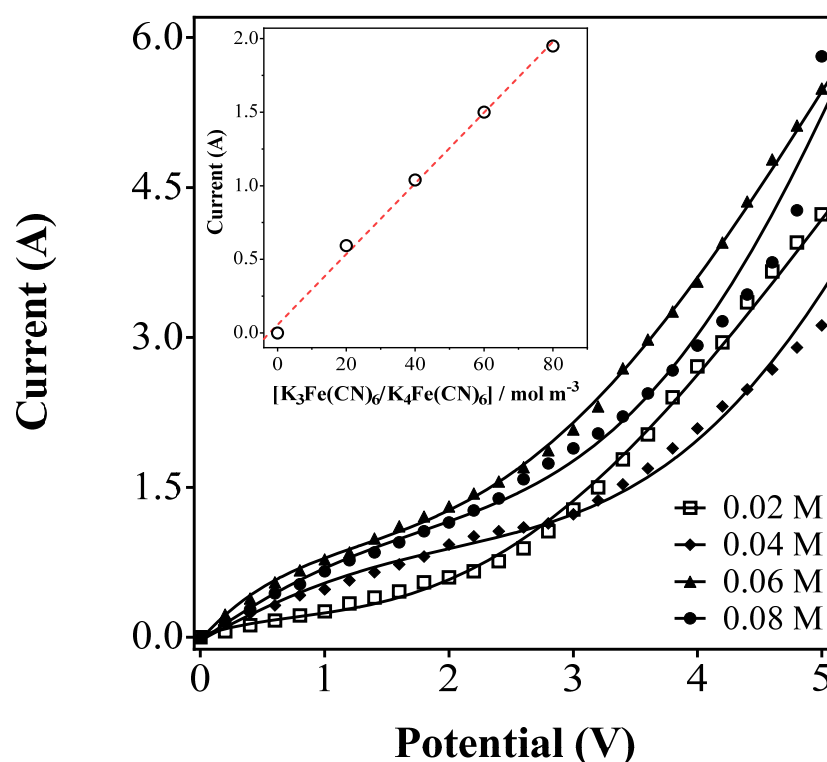


Figure 5. Polarization curves for the mass-transfer characterization of the electrochemical flow cell using 20–80 mol m⁻³ ferricyanide redox couple in 0.5 M NaOH. Inset: variation of limiting current as a function of ferricyanide concentration.

In this frame, the electrochemical treatment was extended to 5 L of polluted-groundwater effluent with Na₂SO₄ (≈0.5 M) using a pilot plant with Ti/RuO₂ double-side anode by applying 30 mA cm⁻² at 25 °C to verify its viability for an industrial scale. As cathodes, two stainless steel plates were used. Figure 6 shows that the degradation of organic matter in the real effluent reached about 68% after 300 min of treatment. This behavior is mainly due to the reaction of the organics in the effluent with •OH at the RuO₂ surface as well as the hydrodynamic conditions of the reactor and the increase in the conductivity by adding Na₂SO₄. By determining COD removal, 87% was achieved, evidencing the effectiveness of SDG 6 electrochemical-based solution to eliminate dissolved organics in groundwater. The concentration of some pollutants after the treatment was efficiently reduced (see Table 3). Discoloration was also achieved by using the pre-pilot plant (Figure 6 and Table 3), giving general information about the elimination of organics from the effluent, especially when dealing with real matrices and/or advanced oxidation/reduction technologies. The chromophore groups, which are part of the molecules responsible for the effluent color, are fragmented during the electrochemical treatment via the participation of oxidizing species, consequently promoting a reduction of the color. However, spectral interferences can be attained during the spectrophotometric measurements due to the formation of intermediates and water matrix components (e.g., natural organic matter, inorganic species), which may absorb radiation at the wavelength of the target organic pollutants. An average of 65% of color abatement is achieved with this methodology of treatment (Table 3), which means that the yellowish color of the wastewater disappears during the 5 h oxidation. However, an increment of SUVA₂₅₄ value occurs, probably due to the difficulty in the removal of recalcitrant aromatic compounds, evidenced by the maintenance of TOC values even with a large COD decrease. This behavior is normal in real wastewater matrices [39,53]. Finally, considering the E_{cell}, electrolysis time (300 min), and COD removal, 2.53 kWh kg COD⁻¹ was necessary to efficiently reduce the concentration of main pollutants and other dissolved organics (see Table 3).

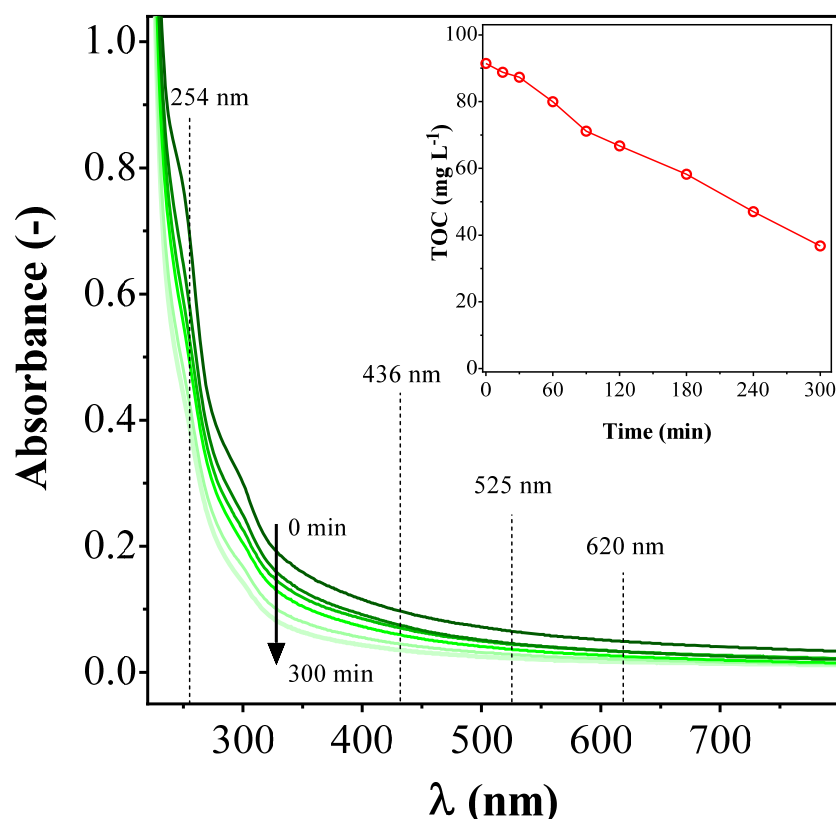


Figure 6. Wavelength spectrum and TOC decay (inset), as a function of time, of 5 L of polluted groundwater effluent by applying 30 mA cm^{-2} at $25 \text{ }^{\circ}\text{C}$ in presence of Na_2SO_4 ($\approx 0.5 \text{ M}$), with the pilot plant with Ti/RuO₂ double-side anode.

Table 3. Physical-chemical characterization after EO treatment at the pre-pilot plant with a Ti/RuO₂ double-sided anode.

Parameter	Before Treatment	After Treatment	MAV ^a
COD ($\text{mg O}_2 \text{ L}^{-1}$)	230	30	-
TOC (mg C L^{-1})	91.5	36.7	-
pH	6.59	6.72	-
Phenol content ($\mu\text{g L}^{-1}$)	6	<1	3
Benzene ($\mu\text{g L}^{-1}$)	96.6	<1.5	5
Toluene ($\mu\text{g L}^{-1}$)	2441	<1.5	170
Ethylbenzene ($\mu\text{g L}^{-1}$)	925.5	<1.5	200
Xylene (<i>o</i> -, <i>p</i> - and <i>m</i> -) ($\mu\text{g L}^{-1}$)	5435.5	500	300
PAHs (mg L^{-1})	4.66	4	-
Color (DFZ at 436, 525, and 620 nm)	9.5; 6.5; 4.9	3.5; 2.2; 1.7	-
Absorbance at 254 nm (AU)	0.714	0.402	-
SUVA ₂₅₄	0.78	1.09	-

Note: ^a Maximum Allowed Value for groundwater (human consumption) based on current legislation in Brazil [34].

4. Conclusions

The electrochemical oxidation treatment of polluted groundwater proposed in this work is proper for the efficient removal of color and organics of major concern from the environment, which is in agreement with SDG 6 (i.e., depollution of water, sanitation, dis-

infection, water treatment, as well as their specialized use for monitoring pollutants) [8,54]. The comparative analysis of organics removal of effluent was performed by employing three different anodes (Ti, Ru, and BDD) while varying the current density, in addition to the use of Na₂SO₄ as an electrolyte. Less energy consumption was identified with the Ti/RuO₂ anode, besides higher mineralization. In this way, the viability of industrial-scale treatment of water with the same characteristics as shown in this work is demonstrated by employing a pre-pilot with a Ti/RuO₂ double-sided anode, 0.5 M of Na₂SO₄ as the electrolyte, and at 30 mA cm⁻² (25 °C, 5 h treatment). With these characteristics, 87% of COD abatement was achieved, mineralization of almost 40% through TOC analysis, and abatement of 65% of color. The BTEX compounds concentration was lowered to values authorized by the Brazilian environmental legislations, with exception of xylene, which decreased by 90% but requires a longer reaction time for fulfillment of the normative legislation for human consumption.

Author Contributions: Conceptualization, D.R.d.S.; E.V.d.S.; C.A.M.-H.; methodology, J.C.O.d.S.; A.M.S.S.; I.D.B.S.; formal analysis, J.C.O.d.S.; A.M.S.S.; E.V.d.S. and C.A.M.-H.; investigation J.C.O.d.S.; A.M.S.S.; D.R.d.S.; E.V.d.S.; C.A.M.-H.; resources, C.A.M.-H.; data curation, J.C.O.d.S.; E.V.d.S.; D.R.d.S. and C.A.M.-H.; writing—original draft preparation, J.C.O.d.S.; A.M.S.S.; I.D.B.S.; E.V.d.S. and C.A.M.-H.; writing—review and editing, J.C.O.d.S.; A.M.S.S.; E.V.d.S. and C.A.M.-H.; funding acquisition, E.V.d.S. and C.A.M.-H. All authors have read and agreed to the published version of the manuscript.

Funding: Conselho Nacional de Desenvolvimento Científico e Tecnológico (CNPq, Brazil) (306323/2018-4, 312595/2019-0, 439344/2018-2, 150933/2021-5). Fundação de Amparo à Pesquisa do Estado de São Paulo (Brazil), FAPESP 2014/50945-4 and 2019/13113-4. Alexander von Humboldt Foundation (Germany) and CAPES (Brazil) 88881.136108/2017-01.

Institutional Review Board Statement: Not applicable.

Informed Consent Statement: Not applicable.

Data Availability Statement: Not applicable.

Acknowledgments: Financial supports from Conselho Nacional de Desenvolvimento Científico e Tecnológico (CNPq, Brazil) (306323/2018-4, 312595/2019-0, 439344/2018-2), and from Fundação de Amparo à Pesquisa do Estado de São Paulo (Brazil), FAPESP 2014/50945-4 and 2019/13113-4, are gratefully acknowledged. Carlos A. Martínez-Huitle acknowledges the funding provided by the Alexander von Humboldt Foundation (Germany) and CAPES (Brazil) as a Humboldt fellowship for Experienced Researcher (88881.136108/2017-01) at the Johannes Gutenberg-Universität Mainz, Germany. Inalmar D. Barbosa Segundo gratefully acknowledges the financial support under post-doctoral grant awarded (CNPq, 150933/2021-5).

Conflicts of Interest: The authors declare no conflict of interest.

References

1. Foster, S.; Chilton, J. Policy experience with groundwater protection from diffuse pollution—A review. *Curr. Opin. Environ. Sci. Health* **2021**, *23*, 100288. [[CrossRef](#)]
2. Yang, Y.; Cheng, Y. Evaluating the ability of transformed urban agglomerations to achieve Sustainable Development Goal 6 from the perspective of the water planet boundary: Evidence from Guanzhong in China. *J. Clean. Prod.* **2021**, *314*, 128038. [[CrossRef](#)]
3. United Nations. *Sustainable Development Goal 6 Synthesis Report 2018 on Water and Sanitation*; United Nations: New York, NY, USA, 2018.
4. Chamanehpour, E.; Sayadi, M.H.; Yousefi, E. The potential evaluation of groundwater pollution based on the intrinsic and the specific vulnerability index. *Groundw. Sustain. Dev.* **2019**, *10*, 100313. [[CrossRef](#)]
5. Ibigbami, O.A.; Adeyeye, E.I.; Adelodun, A.A. Polychlorinated Biphenyls and Polycyclic Aromatic Hydrocarbons in Groundwater of Fuel-Impacted Areas in Ado-Ekiti, Nigeria. *Polycycl. Aromat. Compd.* **2020**, *42*, 2433–2446. [[CrossRef](#)]
6. Liu, S.-H.; Lai, C.-Y.; Ye, J.-W.; Lin, C.-W. Increasing removal of benzene from groundwater using stacked tubular air-cathode microbial fuel cells. *J. Clean. Prod.* **2018**, *194*, 78–84. [[CrossRef](#)]
7. Lien, P.; Yang, Z.; Chang, Y.; Tu, Y.; Kao, C. Enhanced bioremediation of TCE-contaminated groundwater with coexistence of fuel oil: Effectiveness and mechanism study. *Chem. Eng. J.* **2016**, *289*, 525–536. [[CrossRef](#)]
8. Misra, A.K. Climate change and challenges of water and food security. *Int. J. Sustain. Built Environ.* **2014**, *3*, 153–165. [[CrossRef](#)]

9. Mishra, B.K.; Chakraborty, S.; Kumar, P.; Saraswat, C. Correction to: Sustainable Solutions for Urban Water Security. In *Sustainable Solutions for Urban Water Security: Innovative Studies*; Mishra, B.K., Chakraborty, S., Kumar, P., Saraswat, C., Eds.; Springer International Publishing: Cham, Switzerland, 2020; p. C1. ISBN 978-3-030-53110-2.
10. Martínez-Huitle, C.A.; Panizza, M. Electrochemical oxidation of organic pollutants for wastewater treatment. *Curr. Opin. Electrochem.* **2018**, *11*, 62–71. [[CrossRef](#)]
11. Martínez-Huitle, C.A.; Sirés, I.; Rodrigo, M.A. Editorial overview: Electrochemical technologies for wastewater treatment with a bright future in the forthcoming years to benefit of our society. *Curr. Opin. Electrochem.* **2021**, *30*, 100905. [[CrossRef](#)]
12. Ganiyu, S.O.; Martínez-Huitle, C.A. The use of renewable energies driving electrochemical technologies for environmental applications. *Curr. Opin. Electrochem.* **2020**, *22*, 211–220. [[CrossRef](#)]
13. Henrique, J.M.; Monteiro, M.K.; Cardozo, J.C.; Martínez-Huitle, C.A.; da Silva, D.R.; dos Santos, E.V. Integrated-electrochemical approaches powered by photovoltaic energy for detecting and treating paracetamol in water. *J. Electroanal. Chem.* **2020**, *876*, 114734. [[CrossRef](#)]
14. Martínez-Huitle, C.A.; Rodrigo, M.A.; Sirés, I.; Scialdone, O. Single and Coupled Electrochemical Processes and Reactors for the Abatement of Organic Water Pollutants: A Critical Review. *Chem. Rev.* **2015**, *115*, 13362–13407. [[CrossRef](#)] [[PubMed](#)]
15. Panizza, M.; Cerisola, G. Direct And Mediated Anodic Oxidation of Organic Pollutants. *Chem. Rev.* **2009**, *109*, 6541–6569. [[CrossRef](#)] [[PubMed](#)]
16. Brillas, E.; Martínez-Huitle, C.A. Decontamination of wastewaters containing synthetic organic dyes by electrochemical methods. An updated review. *Appl. Catal. B Environ.* **2015**, *166–167*, 603–643. [[CrossRef](#)]
17. Tavares, M.G.; da Silva, L.V.; Solano, A.M.S.; Tonholo, J.; Martínez-Huitle, C.A.; Zanta, C.L. Electrochemical oxidation of Methyl Red using Ti/Ru_{0.3}Ti_{0.7}O₂ and Ti/Pt anodes. *Chem. Eng. J.* **2012**, *204–206*, 141–150. [[CrossRef](#)]
18. Solano, A.M.S.; Martínez-Huitle, C.A.; Garcia-Segura, S.; El-Ghenymy, A.; Brillas, E. Application of electrochemical advanced oxidation processes with a boron-doped diamond anode to degrade acidic solutions of Reactive Blue 15 (Turquoise Blue) dye. *Electrochim. Acta* **2016**, *197*, 210–220. [[CrossRef](#)]
19. Martínez-Huitle, C.A.; Brillas, E. A critical review over the electrochemical disinfection of bacteria in synthetic and real wastewaters using a boron-doped diamond anode. *Curr. Opin. Solid State Mater. Sci.* **2021**, *25*, 100926. [[CrossRef](#)]
20. Ganiyu, S.O.; Martínez-Huitle, C.A.; Oturan, M.A. Electrochemical advanced oxidation processes for wastewater treatment: Advances in formation and detection of reactive species and mechanisms. *Curr. Opin. Electrochem.* **2020**, *27*, 100678. [[CrossRef](#)]
21. Bergmann, H. Electrochemical disinfection—State of the art and tendencies. *Curr. Opin. Electrochem.* **2021**, *28*, 100694. [[CrossRef](#)]
22. Escalona-Durán, F.; da Silva, D.R.; Martínez-Huitle, C.A.; Villegas-Guzman, P. The synergic persulfate-sodium dodecyl sulfate effect during the electro-oxidation of caffeine using active and non-active anodes. *Chemosphere* **2020**, *253*, 126599. [[CrossRef](#)]
23. Chaplin, B.P. The Prospect of Electrochemical Technologies Advancing Worldwide Water Treatment. *Accounts Chem. Res.* **2019**, *52*, 596–604. [[CrossRef](#)] [[PubMed](#)]
24. Ganiyu, S.O.; Martínez-Huitle, C.A. Nature, Mechanisms and Reactivity of Electrogenenerated Reactive Species at Thin-Film Boron-Doped Diamond (BDD) Electrodes During Electrochemical Wastewater Treatment. *ChemElectroChem* **2019**, *6*, 2379–2392. [[CrossRef](#)]
25. Nidheesh, P.V.; Divyapriya, G.; Oturan, N.; Trellu, C.; Oturan, M.A. Environmental Applications of Boron-Doped Diamond Electrodes: 1. Applications in Water and Wastewater Treatment. *ChemElectroChem* **2019**, *6*, 2124–2142. [[CrossRef](#)]
26. He, Y.; Lin, H.; Guo, Z.; Zhang, W.; Li, H.; Huang, W. Recent developments and advances in boron-doped diamond electrodes for electrochemical oxidation of organic pollutants. *Sep. Purif. Technol.* **2018**, *212*, 802–821. [[CrossRef](#)]
27. Du, X.; Oturan, M.A.; Zhou, M.; Belkessa, N.; Su, P.; Cai, J.; Trellu, C.; Mousset, E. Nanostructured electrodes for electrocatalytic advanced oxidation processes: From materials preparation to mechanisms understanding and wastewater treatment applications. *Appl. Catal. B Environ.* **2021**, *296*, 120332. [[CrossRef](#)]
28. Pérez, J.; Llanos, J.; Sáez, C.; López, C.; Cañizares, P.; Rodrigo, M. Development of an innovative approach for low-impact wastewater treatment: A microfluidic flow-through electrochemical reactor. *Chem. Eng. J.* **2018**, *351*, 766–772. [[CrossRef](#)]
29. Yang, N.; Yu, S.; Macpherson, J.V.; Einaga, Y.; Zhao, H.; Zhao, G.; Swain, G.M.; Jiang, X. Conductive diamond: Synthesis, properties, and electrochemical applications. *Chem. Soc. Rev.* **2018**, *48*, 157–204. [[CrossRef](#)]
30. Manan, T.S.B.A.; Khan, T.; Mohtar, W.H.M.W.; Beddu, S.; Kamal, N.L.M.; Yavari, S.; Jusoh, H.; Qazi, S.; Supaat, S.K.B.I.; Adnan, F.; et al. Dataset on specific UV absorbances (SUVA₂₅₄) at stretch components of Perak River basin. *Data Brief* **2020**, *30*, 105518. [[CrossRef](#)]
31. German Institute for Standardization. Water Quality - Examination and Determination of Colour (ISO 7887:2012-04), 2012. Available online: https://shop.standards.ie/en-ie/standards/din-en-iso-7887-2012-04-399902_saig_din_din_875612/ (accessed on 9 September 2022).
32. Martínez-Huitle, C.A.; Quiroz, M.A.; Comninellis, C.; Ferro, S.; De Battisti, A. Electrochemical incineration of chloranilic acid using Ti/IrO₂, Pb/PbO₂ and Si/BDD electrodes. *Electrochim. Acta* **2004**, *50*, 949–956. [[CrossRef](#)]
33. Moreira, F.C.; Boaventura, R.A.R.; Brillas, E.; Vilar, V.J.P. Electrochemical advanced oxidation processes: A review on their application to synthetic and real wastewaters. *Appl. Catal. B Environ.* **2017**, *202*, 217–261. [[CrossRef](#)]
34. Brazilian National Council of the Environment. Resolution Number 396, 3 April 2008. Available online: <https://www.braziannr.com/brazilian-environmental-legislation/conama-resolution-39608/> (accessed on 9 September 2022).

35. Cardozo, J.C.; da Silva, D.R.; Martínez-Huitle, C.A.; Quiroz, M.A.; dos Santos, E.V. The versatile behavior of diamond electrodes—Electrochemical examination of the anti-psychotic drug olanzapine (OL) oxidation as a model organic aqueous solution. *Electrochim. Acta* **2022**, *411*, 140063. [[CrossRef](#)]
36. Ganiyu, S.O.; dos Santos, E.V.; Martínez-Huitle, C.A.; Waldvogel, S.R. Opportunities and challenges of thin-film boron-doped diamond electrochemistry for valuable resources recovery from waste: Organic, inorganic, and volatile product electrosynthesis. *Curr. Opin. Electrochem.* **2021**, *32*, 100903. [[CrossRef](#)]
37. Panizza, M.; Cerisola, G. Applicability of electrochemical methods to carwash wastewaters for reuse. Part 1: Anodic oxidation with diamond and lead dioxide anodes. *J. Electroanal. Chem.* **2010**, *638*, 28–32. [[CrossRef](#)]
38. Ganiyu, S.O.; dos Santos, E.V.; Costa, E.C.T.D.A.; Martínez-Huitle, C.A. Electrochemical advanced oxidation processes (EAOPs) as alternative treatment techniques for carwash wastewater reclamation. *Chemosphere* **2018**, *211*, 998–1006. [[CrossRef](#)]
39. Segundo, I.D.B.; Martins, R.J.; Boaventura, R.A.; Silva, T.F.; Moreira, F.C.; Vilar, V.J. Finding a suitable treatment solution for a leachate from a non-hazardous industrial solid waste landfill. *J. Environ. Chem. Eng.* **2021**, *9*, 105168. [[CrossRef](#)]
40. Brito, L.R.; Ganiyu, S.O.; dos Santos, E.V.; Oturan, M.A.; Martínez-Huitle, C.A. Removal of antibiotic rifampicin from aqueous media by advanced electrochemical oxidation: Role of electrode materials, electrolytes and real water matrices. *Electrochim. Acta* **2021**, *396*, 139254. [[CrossRef](#)]
41. Solano, A.M.S.; de Araújo, C.K.C.; de Melo, J.V.; Peralta-Hernandez, J.M.; da Silva, D.R.; Martínez-Huitle, C.A. Decontamination of real textile industrial effluent by strong oxidant species electrogenerated on diamond electrode: Viability and disadvantages of this electrochemical technology. *Appl. Catal. B Environ.* **2012**, *130–131*, 112–120. [[CrossRef](#)]
42. de Moura, D.C.; Brito, C.D.N.; Quiroz, M.A.; Pergher, S.; Martinez-Huitle, C.A. Cl-mediated electrochemical oxidation for treating an effluent using platinum and diamond anodes. *J. Water Process Eng.* **2015**, *8*, e31–e36. [[CrossRef](#)]
43. Sirés, I.; Brillas, E.; Oturan, M.A.; Rodrigo, M.A.; Panizza, M. Electrochemical Advanced Oxidation Processes: Today and Tomorrow. A Review. *Environ. Sci. Pollut. Res.* **2014**, *21*, 8336–8367. [[CrossRef](#)]
44. Divyapriya, G.; Nidheesh, P. Electrochemically generated sulfate radicals by boron doped diamond and its environmental applications. *Curr. Opin. Solid State Mater. Sci.* **2021**, *25*, 100921. [[CrossRef](#)]
45. Barreto, J.P.D.P.; Araújo, K.; de Araújo, D.M.; Martinez-Huitle, C.A. Effect of sp³/sp² Ratio on Boron Doped Diamond Films for Producing Persulfate. *ECS Electrochem. Lett.* **2015**, *4*, E9–E11. [[CrossRef](#)]
46. Araújo, K.C.D.F.; da Silva, D.R.; dos Santos, E.V.; Varela, H.; Martínez-Huitle, C.A. Investigation of persulfate production on BDD anode by understanding the impact of water concentration. *J. Electroanal. Chem.* **2020**, *860*, 113927. [[CrossRef](#)]
47. Srivastava, V.; Kumar, M.S.; Nidheesh, P.V.; Martínez-Huitle, C.A. Electro catalytic generation of reactive species at diamond electrodes and applications in microbial inactivation. *Curr. Opin. Electrochem.* **2021**, *30*, 100849. [[CrossRef](#)]
48. Serrano, K.G. A critical review on the electrochemical production and use of peroxo-compounds. *Curr. Opin. Electrochem.* **2020**, *27*, 100679. [[CrossRef](#)]
49. Scaria, J.; Nidheesh, P.V. Comparison of hydroxyl-radical-based advanced oxidation processes with sulfate radical-based advanced oxidation processes. *Curr. Opin. Chem. Eng.* **2022**, *36*, 100830. [[CrossRef](#)]
50. Divyapriya, G.; Singh, S.; Martínez-Huitle, C.A.; Scaria, J.; Karim, A.V.; Nidheesh, P. Treatment of real wastewater by photoelectrochemical methods: An overview. *Chemosphere* **2021**, *276*, 130188. [[CrossRef](#)]
51. Ferreira, M.B.; Solano, A.M.S.; Dos Santos, E.V.; Martínez-Huitle, C.A.; Ganiyu, S.O. Coupling of Anodic Oxidation and Soil Remediation Processes: A Review. *Materials* **2020**, *13*, 4309. [[CrossRef](#)]
52. Ganiyu, S.O.; El-Din, M.G. Insight into in-situ radical and non-radical oxidative degradation of organic compounds in complex real matrix during electrooxidation with boron doped diamond electrode: A case study of oil sands process water treatment. *Appl. Catal. B Environ.* **2020**, *279*, 119366. [[CrossRef](#)]
53. Segundo, I.D.B.; Moreira, F.C.; Silva, T.F.; Weblar, A.D.; Boaventura, R.A.; Vilar, V.J. Development of a treatment train for the remediation of a hazardous industrial waste landfill leachate: A big challenge. *Sci. Total Environ.* **2020**, *741*, 140165. [[CrossRef](#)]
54. Mishra, B.K.; Chakraborty, S.; Kumar, P.; Saraswat, C. *Sustainable Solutions for Urban Water Security*; Springer International Publishing: New York, NY, USA, 2020. [[CrossRef](#)]